

## Electronic Supplementary Information

### Colloidal Syntheses of Zero-Dimensional Cs<sub>4</sub>SnX<sub>6</sub> (X = Br, I) Nanocrystals with High Emission Efficiencies

Li Tan,<sup>a</sup> Wu Wang,<sup>b</sup> Qian Li,<sup>a,c</sup> Zhishan Luo,<sup>a,c</sup> Chao Zou,<sup>a</sup> Min Tang,<sup>a</sup> Liming Zhang,<sup>a</sup> Jiaqing He,<sup>b</sup> and Zewei Quan<sup>\*a</sup>

<sup>a</sup> Department of Chemistry, Southern University of Science and Technology (SUSTech), Shenzhen, Guangdong 518055, China

<sup>b</sup> Department of Physics, Southern University of Science and Technology (SUSTech), Shenzhen, Guangdong 518055, China

<sup>c</sup> Academy for Advanced Interdisciplinary Studies, Southern University of Science and Technology (SUSTech), Shenzhen, Guangdong 518055, China

\* Corresponding author

E-mail: [quanzw@sustech.edu.cn](mailto:quanzw@sustech.edu.cn)

## Part I: Materials and Sample Preparation

### Chemicals

1-octadecene (ODE, 90%), tri-*n*-octylphosphine (TOP), oleylamine (OLA, >70%), oleic acid (OA, 90%) were purchased from Sigma-Aldrich. Tin (II) bromide ( $\text{SnBr}_2$ , 99.2 %) and Tin (II) iodide ( $\text{SnI}_2$ , 99+ %) were purchased from Alfa. Cesium carbonate ( $\text{Cs}_2\text{CO}_3$ , 99.99%) was purchased from Aladdin. All chemicals were stored in an air-free, Ar-filled glovebox with  $\text{O}_2$  and  $\text{H}_2\text{O}$  level < 0.5 ppm, and were used as received without any further purification.

### Syntheses of phase-pure $\text{Cs}_4\text{SnX}_6$ (X = Br, I) NCs

8 mg of  $\text{Cs}_2\text{CO}_3$  was loaded in a three-necked Schlenk flask and sealed in a glovebox, and then 5 mL of ODE was injected into the flask, followed by the addition of 0.1 mL of OA and 0.1 mL of OLA. The flask was then degassed under vacuum for 1 h at 115 °C. Subsequently, the reaction was heated to the chosen reaction temperature before the desired amount of  $\text{SnX}_2$  dissolved in 0.5 mL of TOP was swiftly injected into the prepared Cs-precursor. The reaction vessel was kept at the injection temperature for appropriate time, followed by cooling down to room temperature by using a water bath. Finally, NCs were collected via centrifugation at 10000 rpm for 5 min, and then the samples were immediately stored in glovebox.

For the preparation of  $\text{Cs}_4\text{SnBr}_6$  NCs, 60 mg of  $\text{SnBr}_2$  was used, and the reaction was conducted at 210 °C for 1 min. For the mixed halide NCs, 45 mg of  $\text{SnBr}_2$  and 17.5 mg of  $\text{SnI}_2$  were used to initiate the reaction, and the reaction was performed at 210 °C for 1 min. To synthesize  $\text{Cs}_4\text{SnI}_6$  NCs, 70 mg of  $\text{SnI}_2$  was dissolved in TOP, and the reaction temperature was set to 250 °C to obtain a pure phase. Instead of 1 min reaction, 15 s was used to obtain monodisperse  $\text{Cs}_4\text{SnI}_6$  NCs.

## Part II: Characterizations Methods and Calculation Details

### Characterizations

Transmission electron microscopy (TEM) measurement was performed in Hitachi HT7700 microscope operated at 100 kV to investigate the sizes and morphologies of  $\text{Cs}_4\text{SnX}_6$  NCs. The

microstructures of the Cs<sub>4</sub>SnX<sub>6</sub> samples were characterized by high-resolution transmission electron microscopy (HRTEM) and selected area electron diffraction (SAED), and their chemical composition were analyzed by energy dispersive X-ray spectroscopy (EDX) under scanning transmission electron microscopy (STEM) mode using the Super-X EDS detector in a double Cs-corrected FEI Themis G2 60-300 microscope operated at 60 kV. Analyses of STEM-EDX images were carried out by using the Velox software. The sizes of the Cs<sub>4</sub>SnX<sub>6</sub> NCs were estimated from TEM images using Nano Measurer software with ~200 particles statistics.

X-ray diffraction (XRD) patterns were recorded on an X-ray diffractometer (Rigaku SmartLab) with Cu K $\alpha$  radiation ( $\lambda = 0.15418$  nm) at a voltage of 45 kV and a current of 200 mA.

X-ray photoelectron spectroscopy (XPS) analyses were carried out on a PHI 5000 VersaProbe III spectrometer using monochromatic Al K(alpha) X-ray source. XPS samples were prepared in an argon filled glove box (O<sub>2</sub>, H<sub>2</sub>O < 0.5 ppm) and transferred to an ultrahigh vacuum chamber.

Raman spectra were measured by using the Raman spectrometer of HORIBA iHR550 with 532 nm laser.

The UV-Vis absorption spectra were measured with Agilent Technologies Cary Series UV-Vis-NIR Spectrophotometer in the range of 200-800 nm. The Photoluminescence (PL) and PL excitation spectra were taken by HORIBA Scientific FluoroMax-4 Spectrofluorometer. For Cs<sub>4</sub>SnBr<sub>6</sub> NCs and Cs<sub>4</sub>SnBr<sub>x</sub>I<sub>6-x</sub> NCs, the excitation wavelength was 320 nm, and the excitation wavelength for Cs<sub>4</sub>SnI<sub>6</sub> NCs was 360 nm. PL lifetime measurements were performed by using the Edinburgh Instruments FLS 980-Laser Flash Photolysis Spectrometer correlated single photo counting method with a  $\mu$ F2 light source. The PL decay curves were fitted by using U11487 Software from Hamamatsu Photonics, and the average radiative lifetimes were determined by

$$\tau_{avg} = (\sum_{i=1}^2 \tau_i^2 A_i) / (\sum_{i=1}^2 \tau_i A_i),$$

where  $A_i$  and  $\tau_i$  are the corresponding amplitudes and exponential decay parameters in a bi-exponential analysis. The absolute luminescent quantum yields (PLQY) were recorded with Hamamatsu absolute PL quantum yield spectrometer C11347.

### First-Principle Calculations

Theoretical calculations of band structure and partial density of state (PDOS) were performed using Materials Studio 5.5 program, with generalized gradient approximation (GGA)-perdew-burke-ernzerhof (PBE) functions as implemented in the CASTEP package.<sup>1</sup> During calculation, the plane waves kinetic energy cut off and grid density were chosen as 280 eV and  $48 \times 48 \times 48$ , respectively, and the convergence tolerance between optimization cycles was set as energy change with  $5.0 \times 10^{-7}$  eV/atm. Meanwhile, the ion-electron interactions were modeled by the ultrasoft pseudopotential for all the elements.

### Part III: Supplementary Figures and Tables

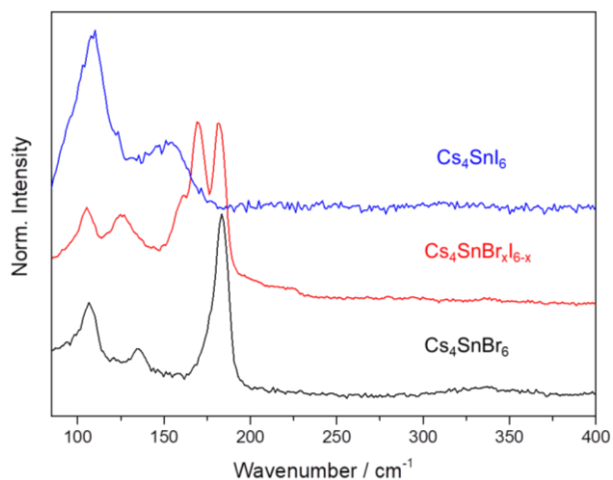


**Fig. S1** Raman spectra of as-prepared Cs<sub>4</sub>SnBr<sub>6</sub> NCs, Cs<sub>4</sub>SnBr<sub>x</sub>I<sub>6-x</sub> NCs and Cs<sub>4</sub>SnI<sub>6</sub> NCs, showing Sn-X vibrations of [SnX<sub>6</sub>]<sup>4-</sup> octahedra.

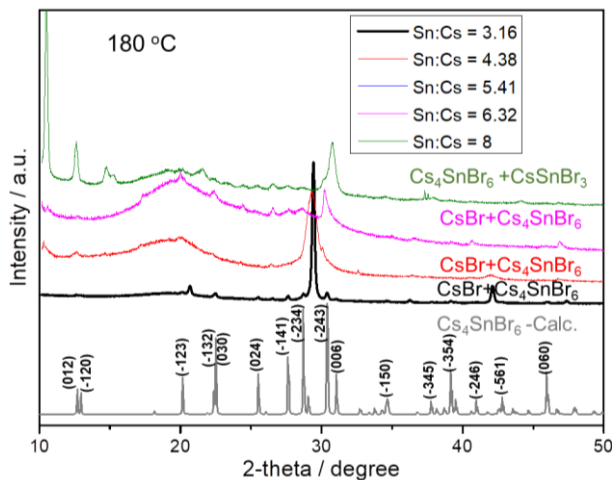


**Fig. S2** XRD patterns of  $\text{Cs}_4\text{SnBr}_6$  NCs synthesized at 180 °C with different Sn/Cs ratios. Note: CsBr and  $\text{CsSnBr}_3$  impurities are observed.

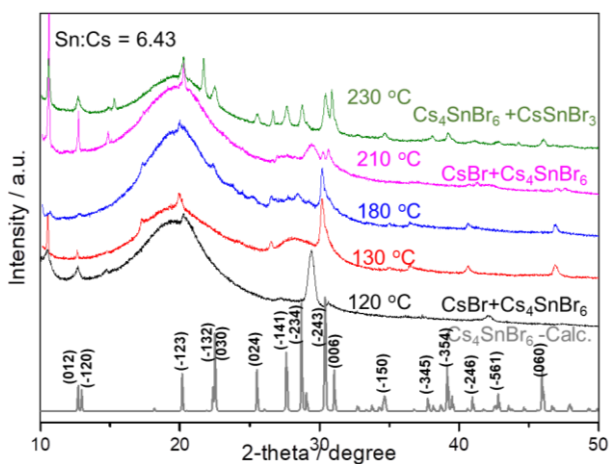


**Fig. S3** XRD patterns of  $\text{Cs}_4\text{SnBr}_6$  NCs synthesized at different temperatures with the Sn/Cs ratio of 6.43. Note: CsBr and  $\text{CsSnBr}_3$  impurities are observed.

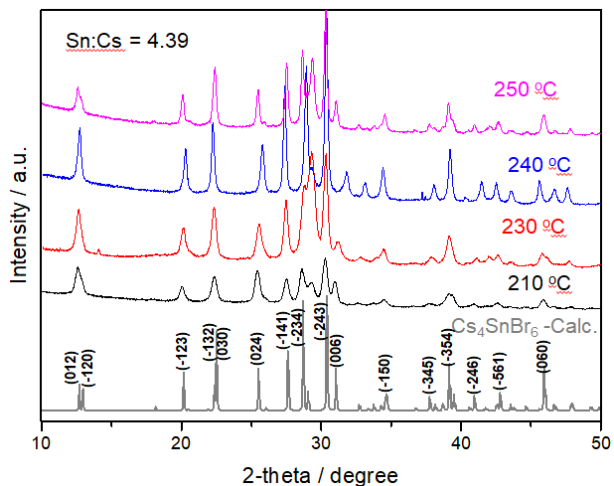


**Fig. S4** XRD patterns of  $\text{Cs}_4\text{SnBr}_6$  NCs synthesized at different temperatures with the Sn/Cs ratio of 4.39.

**Table S1**  $\text{Cs}_4\text{SnX}_6$  (X= Br, I) NC compositions obtained from the quantification of STEM-EDX mapping results.

	$\text{Cs}_4\text{SnBr}_6$	$\text{Cs}_4\text{SnBr}_x\text{I}_{6-x}$	$\text{Cs}_4\text{SnI}_6$
<b>Cs</b>	$33.3 \pm 4.7$ at. %	$28.2 \pm 3.8$ at. %	$38.1 \pm 6.2$ at. %
<b>Sn</b>	$10.2 \pm 1.5$ at. %	$10.5 \pm 1.5$ at. %	$10.9 \pm 1.4$ at. %
<b>Br</b>	$56.6 \pm 5.8$ at. %	$54.6 \pm 5.2$ at. %	—
<b>I</b>	—	$6.6 \pm 0.9$ at. %	$51.0 \pm 8.2$ at. %

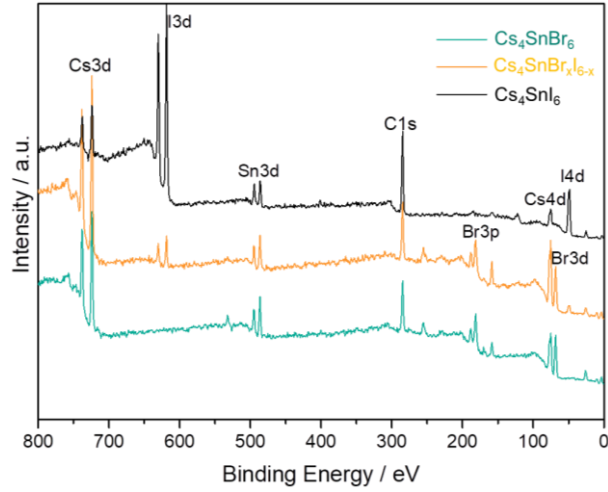


**Fig. S5** XPS survey spectra of  $\text{Cs}_4\text{SnX}_6$  ( $X = \text{Br}, \text{I}$ ) NCs.

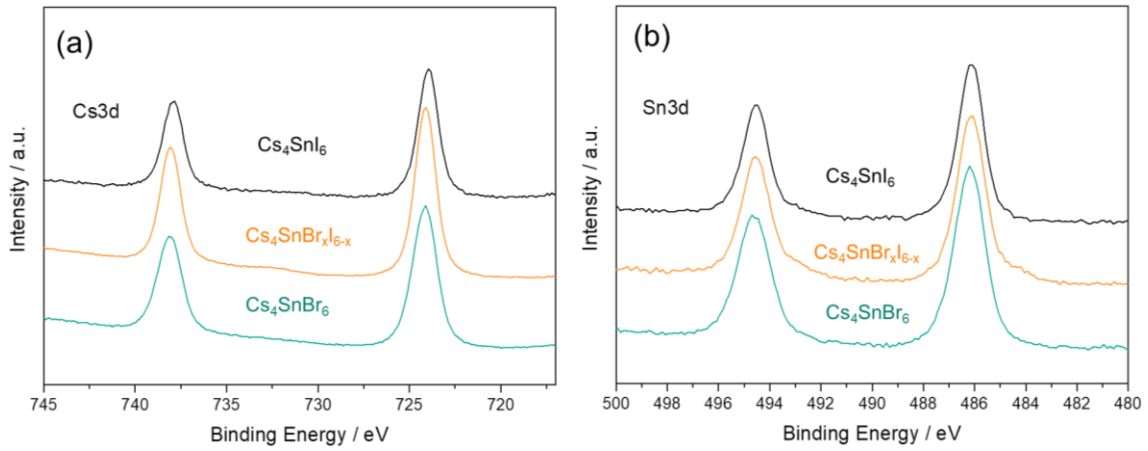


**Fig. S6** XPS spectra of Cs3d (a) and Sn3d (b) of  $\text{Cs}_4\text{SnX}_6$  ( $X = \text{Br}, \text{I}$ ) NCs.

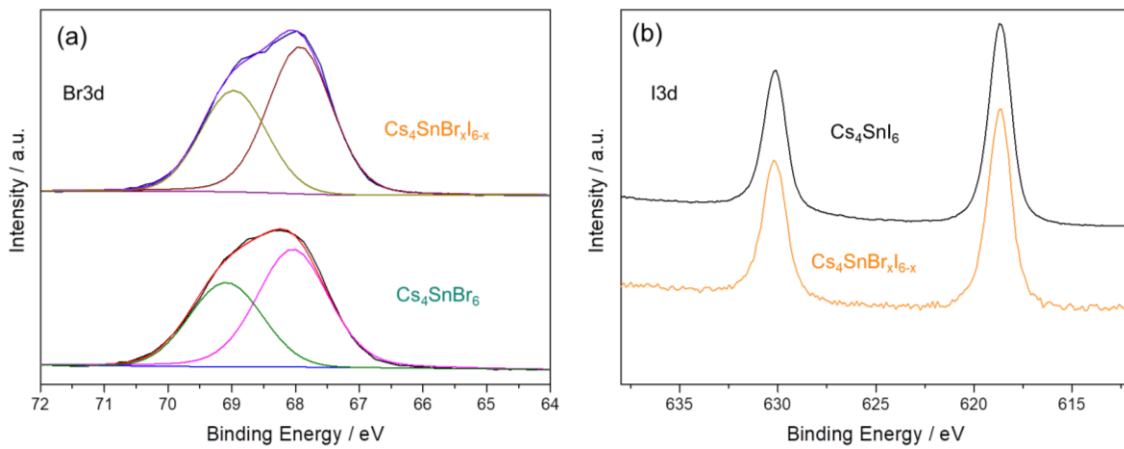


**Fig. S7** XPS spectra of Br3d (a) and I3d (b) of  $\text{Cs}_4\text{SnX}_6$  ( $X = \text{Br}, \text{I}$ ) NCs.

**Table S2** Cs<sub>4</sub>SnX<sub>6</sub> (X= Br, I) NC compositions from the quantification of XPS.

	Cs <sub>4</sub> SnBr <sub>6</sub>	Cs <sub>4</sub> SnBr <sub>x</sub> I <sub>6-x</sub>	Cs <sub>4</sub> SnI <sub>6</sub>
Cs	9.8 at.%	11.98 at.%	4.37 at.%
Sn	2.62 at.%	3.36 at.%	1.39 at.%
Br	14.0 at.%	15.15 at.%	—
I	—	1.77 at.%	7.12 at.%

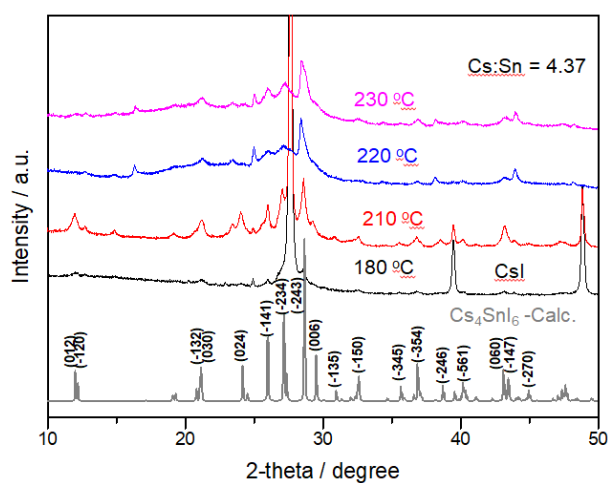


**Fig. S8** XRD patterns of Cs<sub>4</sub>SnI<sub>6</sub> NCs synthesized at different temperatures with the Sn/Cs ratio of 4.37.

Note: CsI is observed.

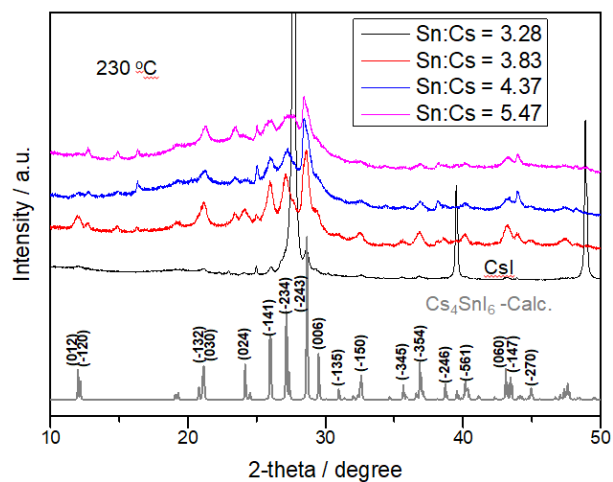


**Fig. S9** XRD patterns of  $\text{Cs}_4\text{SnI}_6$  NCs synthesized at different temperatures with the Sn/Cs ratio of 3.83.

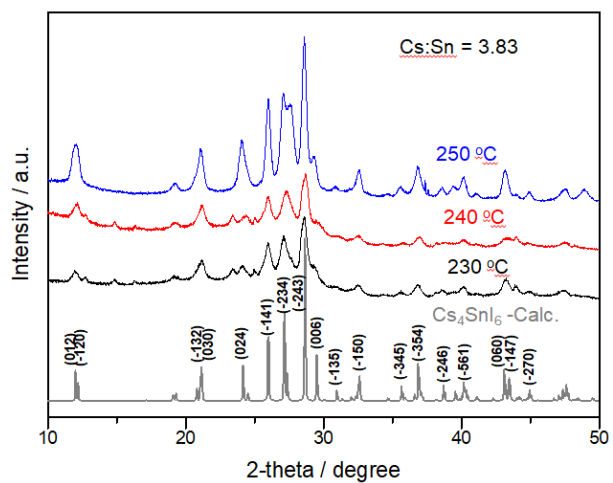


**Fig. S10** XRD patterns of  $\text{Cs}_4\text{SnI}_6$  NCs synthesized at  $230\text{ }^\circ\text{C}$  with different Sn/Cs ratios. Note:  $\text{CsI}$  is observed.

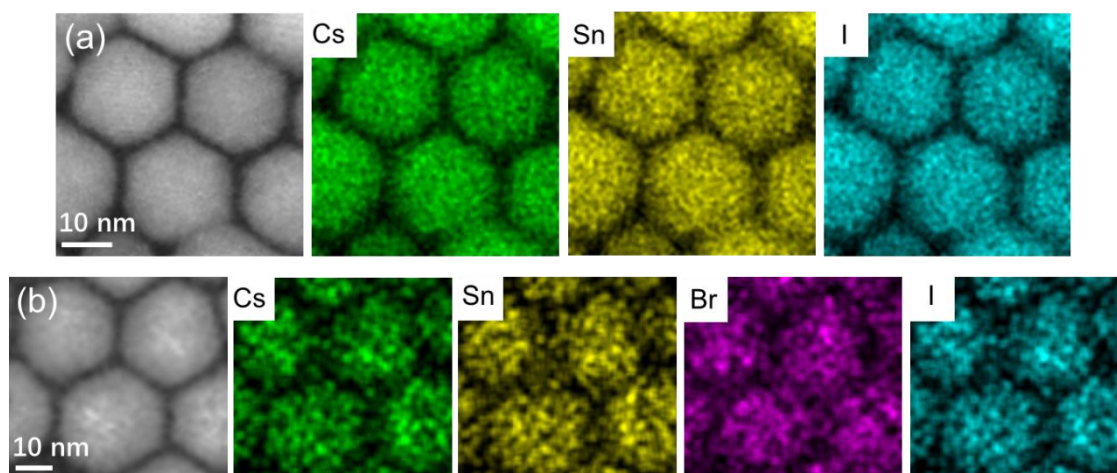


**Fig. S11** STEM-EDX mapping results of Cs<sub>4</sub>SnI<sub>6</sub> NCs (a) and Cs<sub>4</sub>SnBr<sub>x</sub>I<sub>6-x</sub> NCs (b).

**Table S3** Overview of optical characterizations of Cs<sub>4</sub>SnX<sub>6</sub> (X = Br, I) NCs, including PLQYs, PL emission peaks, FWHM values, Stokes shifts and PL lifetimes. Note: all the values are the average of three measurements from three individual samples.

	PLQY (%)	PL peak (nm)	FWHM (nm)	Stokes Shift (nm)	PL Lifetime (ns)
Cs <sub>4</sub> SnBr <sub>6</sub>	21	534	119	215	737
Cs <sub>4</sub> SnBr <sub>x</sub> I <sub>6-x</sub>	6.6	546	121	227	253
Cs <sub>4</sub> SnI <sub>6</sub>	0.7	578	121	215	13

**Table S4** PLQY comparisons of all-inorganic tin-halide NCs.

	PLQYs
$\text{Cs}_2\text{SnI}_6$ <sup>2</sup>	0.48 % (quantum dots), 0.11 % (nanorods), 0.08% (nanowire), 0.054 % (nanobelts), 0.046 % (nanoplates)
$\text{CsSn}(\text{Br}_{0.5}\text{I}_{0.5})_3$ <sup>3</sup>	0.05 % (nanocubes)
$\text{CsSnBr}_3$ <sup>3,4</sup>	2.1 % (nanocages), 0.14 % (nanocubes)
$\text{CsSnI}_3$ <sup>3</sup>	0.06 % (nanocubes)
$\text{Cs}_4\text{SnX}_6$ (This work)	21.4 % ( $\text{Cs}_4\text{SnBr}_6$ ), 6.6 % ( $\text{Cs}_4\text{SnBr}_x\text{I}_{6-x}$ ), 0.7 % ( $\text{Cs}_4\text{SnI}_6$ )

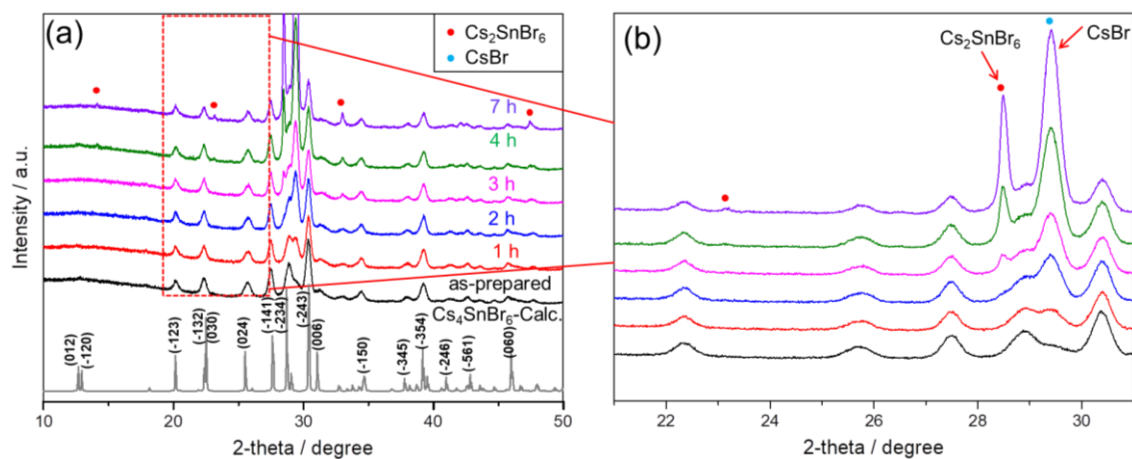


**Fig. S12** XRD patterns of  $\text{Cs}_4\text{SnBr}_6$  NCs after storage in air. (a) The XRD evolutions of  $\text{Cs}_4\text{SnBr}_6$  NCs after storage in air for 1 h, 2 h, 3 h, 4 h and 7 h, showing that  $\text{Cs}_4\text{SnBr}_6$  phase gradually changes into  $\text{Cs}_2\text{SnBr}_6$  and  $\text{CsBr}$ . (b) Enlarged-view of the XRD patterns, indicating the formation of  $\text{CsBr}$  within 1 h and the formation of  $\text{Cs}_2\text{SnBr}_6$  after 2 h.

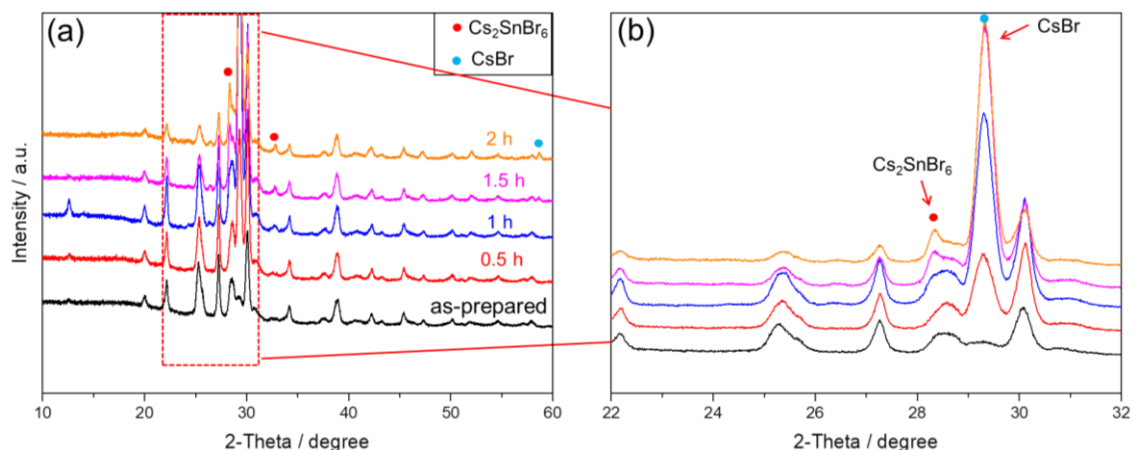


**Fig. S13** XRD patterns of  $\text{Cs}_4\text{SnBr}_x\text{I}_{6-x}$  NCs after storage in air. (a) The XRD evolutions of  $\text{Cs}_4\text{SnBr}_x\text{I}_{6-x}$  NCs after storage in air for 0.5 h, 1 h, 1.5 h and 2 h, showing that  $\text{Cs}_4\text{SnBr}_x\text{I}_{6-x}$  phase gradually changes into  $\text{Cs}_2\text{SnBr}_6$  and CsBr. (b) Enlarged-view of the XRD patterns, indicating the formation of CsBr and  $\text{Cs}_2\text{SnBr}_6$  within 1 h. Note: the Br/I ratio in  $\text{Cs}_4\text{SnBr}_x\text{I}_{6-x}$  NCs is around 9:1, and thus  $\text{Cs}_2\text{SnBr}_6$  and CsBr compounds are easily observed.

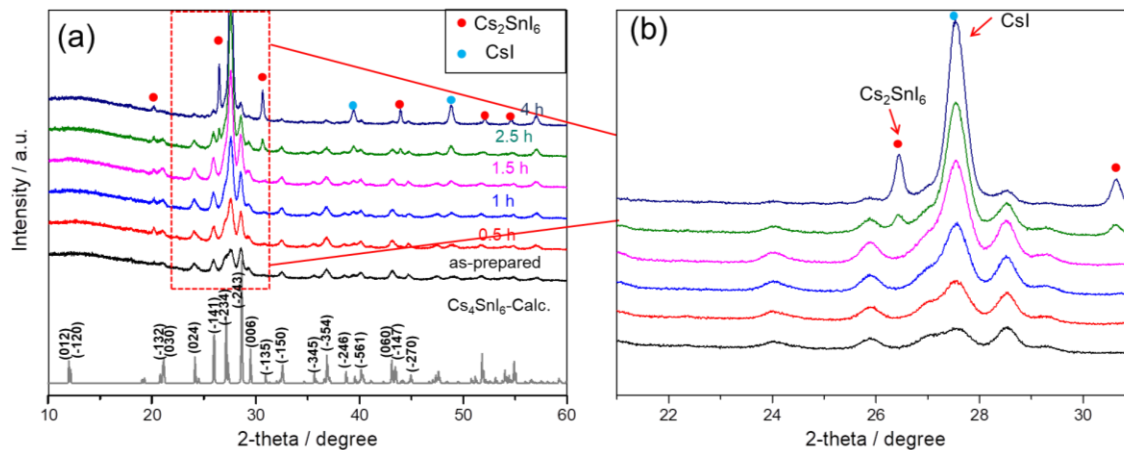


**Fig. S14** XRD patterns of  $\text{Cs}_4\text{SnI}_6$  NCs after storage in air. (a) The XRD evolutions of  $\text{Cs}_4\text{SnI}_6$  NCs after storage in air for 0.5 h, 1 h, 1.5 h, 2.5 h, and 4 h, showing that  $\text{Cs}_4\text{SnI}_6$  phase gradually changes into  $\text{Cs}_2\text{SnI}_6$  and CsI. (b) Enlarged-view of the XRD patterns, indicating the formation of CsI and  $\text{Cs}_2\text{SnI}_6$  within half an hour.

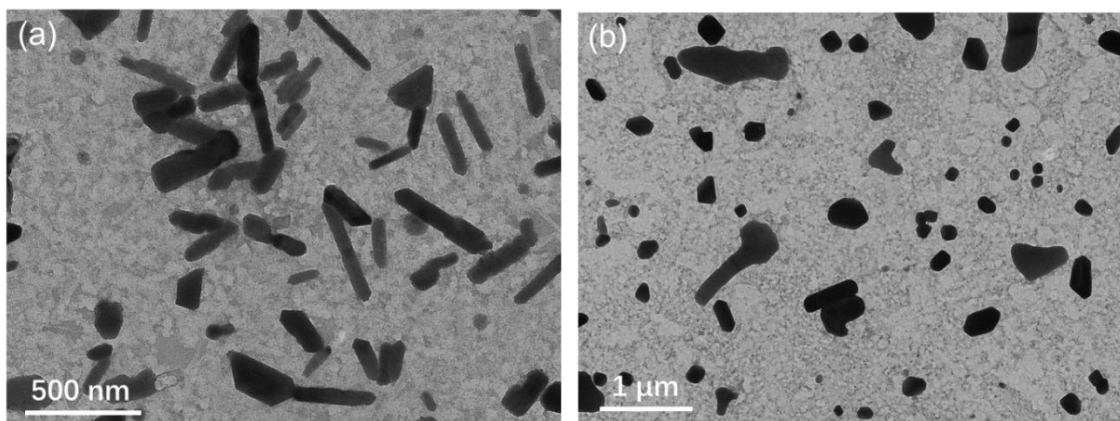


**Fig. S15** TEM images of (a)  $\text{Cs}_4\text{SnBr}_6$  NCs and (b)  $\text{Cs}_4\text{SnI}_6$  NCs after storage in air for 1 week.

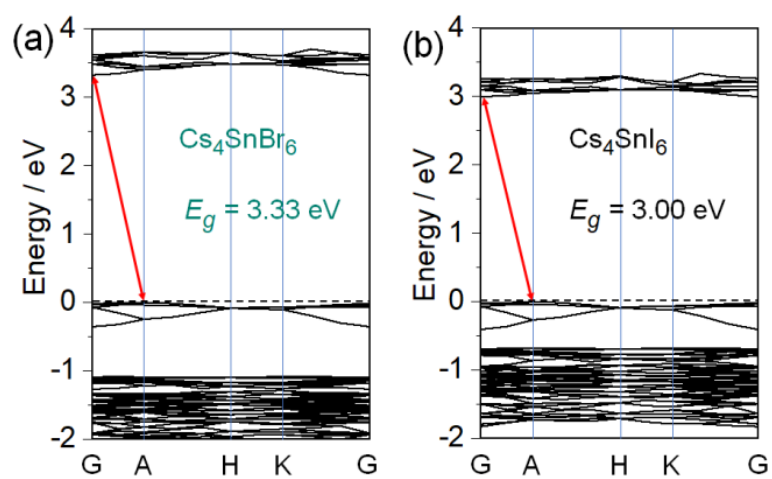


**Fig. S16** Electronic band structures of (a)  $\text{Cs}_4\text{SnBr}_6$  and (b)  $\text{Cs}_4\text{SnI}_6$  calculated based on the PBE functions ( $E_g$ , bandgap energy).

## References

1. J. P. Perdew, K. Burke and M. Ernzerhof, *Phys. Rev. Lett.*, 1996, **77**, 3865-3868.
2. A. Wang, X. Yan, M. Zhang, S. Sun, M. Yang, W. Shen, X. Pan, P. Wang and Z. Deng, *Chem. Mater.*, 2016, **28**, 8132-8140.
3. T. C. Jellicoe, J. M. Richter, H. F. J. Glass, M. Tabachnyk, R. Brady, S. E. Dutton, A. Rao, R. H. Friend, D. Credgington, N. C. Greenham and M. L. Böhm, *J. Am. Chem. Soc.*, 2016, **138**, 2941-2944.
4. A. Wang, Y. Guo, F. Muhammad and Z. Deng, *Chem. Mater.*, 2017, **29**, 6493-6501.